LETTER

Mechanical Features of *Plasmodium falciparum* Acyl Carrier Protein in the Delivery of Substrates

Francesco Colizzi,[†] Maurizio Recanatini,[†] and Andrea Cavalli*[,†,‡]

Department of Pharmaceutical Sciences, University of Bologna, Via Belmeloro 6, I-40126 Bologna, Italy, and Department of Drug Discovery and Development, Italian Institute of Technology, Via Morego 30, I-16163 Genova, Italy

Received August 25, 2008

Abstract: The Acyl Carrier Protein (ACP) is a key element in the biosynthesis of fatty acids being responsible for the acyl group shuttling and delivery within a series of related enzymes. The molecular mechanism of the delivery process is poorly known, and its characterization is essential for in-depth understanding the biosynthetic machinery. A steered molecular dynamics approach has been applied to shed light on the putative delivery pathway, suggesting the small α3-helix act as gatekeeper for the transfer process. Preventing the delivery mechanism would be an innovative strategy for the development of pathway-based antimalarial compounds.

Plasmodium falciparum (*Pf*) infections are the most widespread and lethal form of malaria. Despite the centenary effort to eradicate or control the disease, more than one-third of the human population lives in endemic areas with an estimated half-billion of infections annually resulting in about 2 million deaths.[1−3]

The recently disclosed type II fatty acid synthase (FAS-II) pathway of *Pf* is offering attractive targets potentially enabling the discovery and development of efficacious and selective antimalarial agents.[4] The FAS-II system relies on a dissociative process that exploits a series of individual enzymes that are, indeed, structurally different from the multifunctional type I fatty acid synthase (FAS-I) system of humans.[5] A key feature of the FAS-II is the presence of a small (∼9 kDa), acidic, and highly conserved Acyl Carrier Protein (ACP) that shuttles all the acyl intermediates from one enzyme to the other. The acyl substrates are bound to ACP through a flexible arm formed by the serine-bound prosthetic phosphopantetheine (4′-PP) group (Figure 1a).[6] Nevertheless, ACPs are also known to play a fundamental role in numerous other biosynthetic pathways in which acyl transfer steps are required.[7−9] The geometric properties of several conformationally distinct ACPs have been determined by X-ray crystallography and NMR.[10−15] These experimental data have suggested that structural plasticity is an intrinsic feature of this protein family, providing a possible explanation for ACPs' capability of recognizing multiple enzyme partners and transiently delivering the acyl group to the active sites of these enzymes.[16]

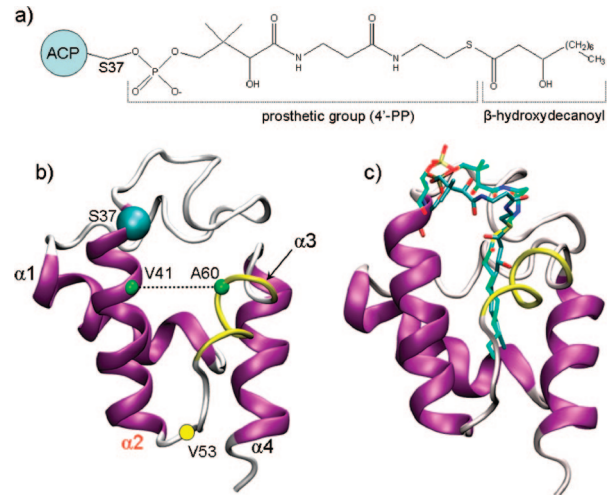

Figure 1. a) 2D structure of the acylated 4′-phosphopantetheine (4′-PP) prosthetic group in the β-hydroxydecanoyl-ACP. b) Overall fold of ACPs; the α3-helix (residues 57−62) is depicted in yellow tube. c) Binding mode of the β-hydroxylated substrate (carbon atoms in cyan) after the MD equilibration compared to the decanoyl substrate (carbon atoms in light green) reported in *E. coli* crystal structure (pdb code: 2fae).

ACP structures are composed of four α-helices delimiting a lipophilic core that forms a binding pocket for fatty acids. Helix α2 has highly conserved residues and plays a major role in ACP-protein interactions (Figure 1b),[17] whereas the short α3-helix does not have a conserved folding among the published ACP structures and, accordingly, this protein portion was observed to experience a helix-loop conformational equilibrium in *Pf*ACP.[14]

Moreover, the analysis of experimental and computational studies suggested the protein region between helices α2 and α4 to be part of the putative ACP/enzyme interface.[18−26]

The functional implication of the above-mentioned structural features is yet unrevealed when observed from the standpoint of the delivery of substrates.

X-ray structures of acylated ACPs have shown the thioester-bound acyl-chain to be embedded into a tunnel-like hydrophobic cavity (Figure 1c), which can harbor acyl substrates of different length.[12,15] Notably, the reactive center of the acyl substrate is buried in the hydrophobic core of the carrier and thus inaccessible to catalytic activities of FAS-II enzymes. Therefore, delivering the substrate from the inner ACP core to the FAS-II enzyme active site is a mandatory event for each biosynthetic step. The molecular understanding of ACP's ability to deliver substrates together with the ability of drug designers to interfere with this process might be a new strategy for the development of innovative FAS-II inhibitors that could behave as pathway modulators rather than single-enzyme inhibitors.

* Corresponding author tel/fax: +39 051 2099735/4; e-mail: andrea.cavalli@unibo.it.
[†] University of Bologna.
[‡] Italian Institute of Technology.

10.1021/ci800297v CCC: $40.75
Published on Web 11/13/2008

Limited structural information about the complex of ACP with biological counterparts and the mechanism of substrate delivery is currently available.[18,27,28] Recently, Leibundgut et al.[27] addressed the delivery issue discussing the crystal structure of the yeast fatty acid synthase (FAS-I type) system with its ACP stalled at one catalytic domain. They have suggested a generic switchblade-like mechanism in which the 4′-PP arm delivers the acyl chain flipping from the ACP core into the catalytic domain active site.[27] However, even though ACPs share the same structural motif in the acyl-substrate binding region, when compared to the FAS-II ACP, the yeast ACP domain (∼18 kDa) has four additional C-terminal α-helices, which take part in the interaction with the catalytic domain. Therefore, differences in the recognition and delivery process between FAS-I and FAS-II systems are likely to occur. Furthermore, substrate delivery is a dynamic process, and the detailed but static X-ray picture requires it to be complemented with other approaches that are able to directly capture the dynamics of the biomolecule under investigation.

In the present work, the dynamics of the delivery mechanism of the β-hydroxydecanoyl substrate by *Pf*ACP was investigated by a Steered Molecular Dynamics (SMD) approach. Analyzing the trajectories and the force profiles, we were able to identify the lowest resistance pathway for the substrate delivery process. In addition, our simulations pointed out both the role of α3-helix as gatekeeper for the substrate transfer process and the effect of the substrate β-hydroxylation on the enzyme recognition.

In SMD simulations, which have been widely and successfully applied to explore the properties of nonequilibrium processes of biomolecules,[29,30] a moving harmonic potential is used to induce a motion along a reaction coordinate. The free end of a virtual spring is moved at constant velocity, while a set of "pulled atoms", attached to the other end of the spring, is subjected to steering forces. The applied forces are determined by the extension of the spring and can be monitored throughout the entire simulation. If the pulled atoms can easily advance along the selected reaction coordinate, the applied force is small and its profile is rather flat. Conversely, if the pulled atoms encounter hindrance along the pathway, the force increases to allow the pulled atoms overcoming energy barriers, thus resulting in quite relevant drops in the force profile. Based on the magnitude of the exerted force, it is possible to determine how easily a pathway can be coursed.[29,30]

The simulations of the covalently bound β-hydroxydecanoyl-ACP complex were performed in explicit water, using the CHARMM[31] force field and the program NAMD[32] [see the Supporting Information (SI) for details]. To get insights into intrinsic properties of the system, the complex was first simulated for 8 ns of unrestrained MD. The average value of rmsd calculated for the backbone along the whole simulation time was 2.9 Å. Nonetheless, the region including residues 53−62 showed high flexibility (RMSf up to 8 Å, red plot in Figure 2a) reflecting the higher ratio of conformational diversity observed by superimposing ACP crystal structures (dotted gray plot in Figure 2a). During the free MD simulations, the β-hydroxyacyl moiety of the bound ligand was floating into the lipophilic core, with the acyl chain maintaining hydrophobic interactions and slightly switching with several extended conformations. Accordingly,

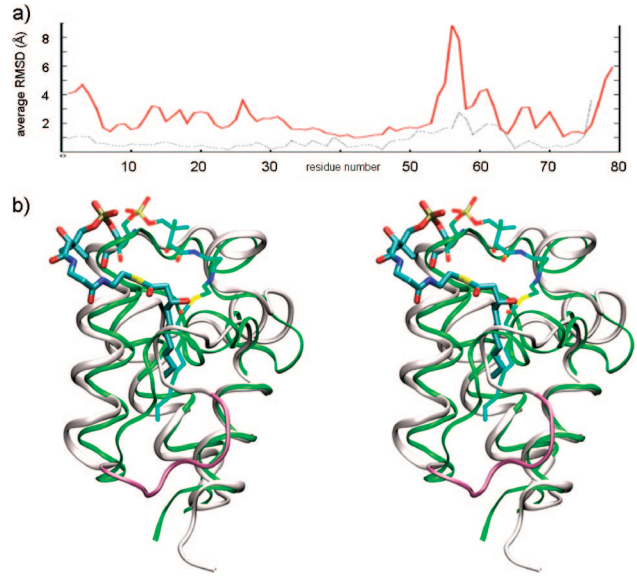

Figure 2. a) Root mean square fluctuation (RMSf) of the *Pf*ACP backbone along the whole MD simulation (red line) and RMSf of up-to-date available crystal structures of *E. coli* ACP after Cα superposition (dotted gray line). b) Stereoview of the β-hydroxydecanoyl-ACP (white ribbon) as it appears after 8 ns of MD. The prosthetic group (cyan) lies on the mouth of the fissure between helices α2 and α3. The highly flexible portion going from 53 to 57 is magenta. The decanoyl-ACP crystal structure (in green, pdb code: 2fae) is shown for comparison.

the presence of multiple low-occupancy conformers is suggested by the electron density map of the decanoyl-ACP crystal structure.[15] The substrate β-hydroxyl group was able to interact with several polar groups (mainly the backbone of D59, A60, and I63) lining the entrance of the ACP binding cavity. As a result, the β-hydroxydecanoyl was less buried in the protein core when compared to the experimentally reported decanoyl analogue. This had the consequence that the prosthetic group (4′-PP) was more relaxed and able to fluctuate among several conformations. Figure 2b shows the prosthetic group protruding toward the solvent, self-docking at the upper fissure between helices α2 and α3. In such a conformation, the FAS-II enzymatic counterparts might still recognize the conserved α2-helix, selectively interact with the prosthetic group, and establish connections with protein segment 53−62. Roujeinikova et al.[15] proposed that the fairly flexible prosthetic arm may adopt a set of different conformations, likely related to the carried acyl substrate, to allow optimal interaction of acyl-ACP intermediates to partner enzymes. However, the MD simulations did not provide any mechanistic explanation of the delivery process. This is likely a consequence of high potential energy barriers implicated, which cannot be sampled by ns-time-scale simulations. To overcome this drawback, we applied SMD (Figure 3) to drive the substrate along several putative reaction coordinates (see Figure 3a).

Combining the ascertainment of available (acyl-)ACPs structures with the critical analysis of the aforementioned experimental data,[18−26] up to ten delivery pathways were initially considered and simulated by means of short time-scale SMD. However, several of them were discarded because either they induced structure unfolding or poorly satisfied the experimental evidence that have suggested helix α2 as a key component of the ACP/enzyme interface (see also the SI).[18−26] Two main putative delivery pathways were

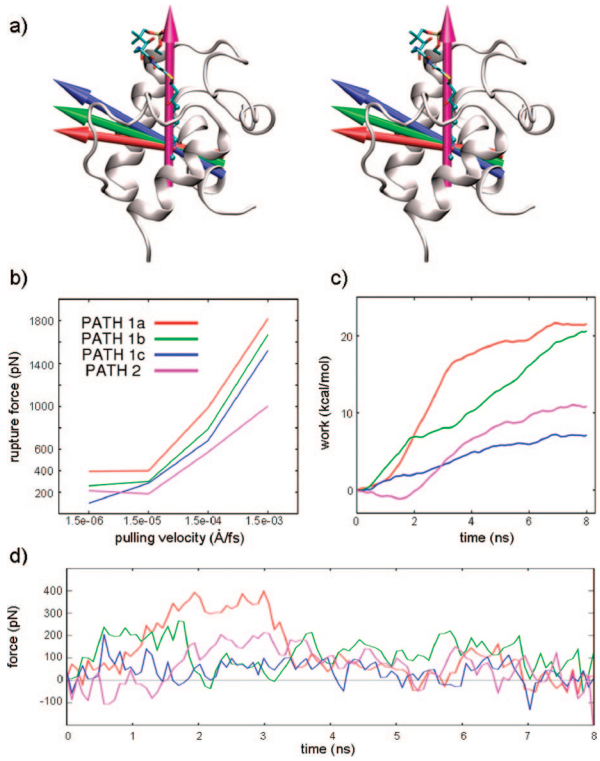

Figure 3. a) Acyl-ACP and the delivery pathways investigated. The arrows represent the pulling directions of the applied forces. b) Correlation of the pulling velocity with the rupture force. At 1.5e-06 Å/fs the process is close to equilibrium. c) Mechanical work done on the system calculated by numerical integration. d) Force profiles of the investigated pathways at 1.5e-06 Å/fs. For sake of clarity the curves are obtained averaging the forces every 30 points.

eventually investigated (Figure 3a): the first one accounting for the substrate exposure through the fissure formed by helices α2 and α3 (path 1); the second one accounting for a sword-unsheathed-like mechanism, in which the substrate is unthreaded away in a parallel direction with respect to the major axis of the binding pocket (path 2). Since for path 1, a protein conformational rearrangement was required, and considering critical the role of the pulling direction, three slightly different subpaths (paths 1a, 1b, and 1c) were investigated. For path 2, preliminary investigations revealed that no relevant protein conformational rearrangements were required and that slight modifications of xyz components of the pulling direction provided very similar force profiles (see the SI). Hence, we assumed that the chosen pulling direction in path 2 was likewise representative of the sword-unsheathed-like mechanism.

In SMD, the pulling velocity (υ) largely influences both the results of simulations and the profile of the applied forces. As υ decreases, the pulled atoms have more time to sample the conformational space and to search for the lowest resistance path along the selected direction. At the same time, the nonpulled atoms can relax following the movement of the pulled atoms, thus reducing the friction rate of the process. As shown in Figure 3b, a lowering of the pulling velocity resulted in a decrease of the observed rupture force likely because of the reduction of nonequilibrium effects.[29,33] Remarkably, at the pulling velocity of 1.5e-06 Å/fs, a plateau was observed, pointing to this pulling rate as the more appropriate one to minimize the friction influence on the delivery process. Such a slow pulling velocity required about

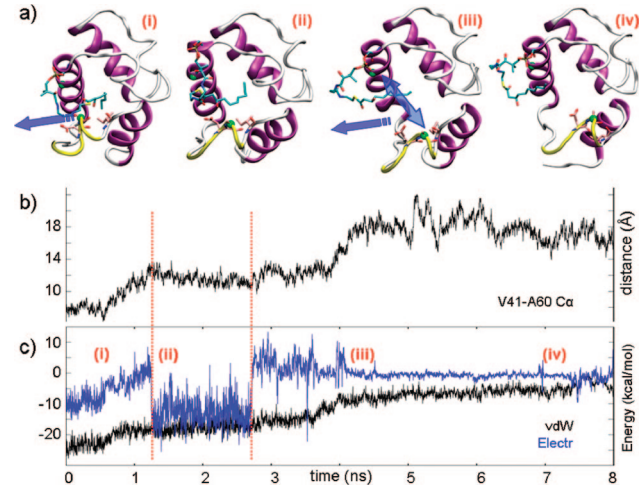

Figure 4. a) Snapshots isolated from the SMD trajectory sampled in path 1c at (i) 300 ps, (ii) 1.6 ns, (iii) 4.2 ns, and (iv) 7 ns. The blue arrow in (i) shows the pulling direction, and in (iii) the double end arrow indicates the opening movement of the fissure formed by helices α2 and α3. b) Evolution of the distance between Cα of V41 and A60. c) Electrostatic and vdW interaction energies between the β-hydroxydecanoyl moiety and the protein residues during the SMD.

8 ns of simulations to allow exposure of the pulled substrate. Using the same simulation time-scale, in the free MD, it was sampled both the partial unfolding of the short α3-helix and the helix folding of residues 19−26 (see the SI). Thus, also in the SMD simulations, some spontaneous conformational changes of ACP could be likely sampled.

In Figure 3d,c, the force profile and the mechanical work done during each simulated pathway are shown, respectively. For each pathway, the force profile correlated well with the rupture and formation of interaction between the outgoing substrate and the binding site residues; a detailed description of the events is reported in the SI.

The system in both paths 1a and 1b encountered relatively high hindrance in the early ns of simulations because the substrate moved against the deep portion of the cleft formed by α2- and α3-helix and lined by the α2-α3 loop. Here, the α3-helix could not spontaneously follow the pulled atoms, and as a consequence the exerted force increased.

In path 1c [Figures 3 (blue line) and 4], the force profile was much flatter than in paths 1a and 1b. We observed an initial force peak (∼200 pN, Figure 3d) due to the breaking of an H-bond network involving the substrate β-OH and the backbone oxygen of A60 and I63. Then, the whole process evolved with a force less than 100 pN. A strong electrostatic interaction involving the β-OH group and the side chain of D59 occurred between ∼1.5−2.5 ns (Figure 4c). Concertedly, a slow "gate opening" was manifested by the increasing distance between V41 and A60 (see also Figure 1b). The flatness of the applied force profile indicated that both the pulled substrate and the constraint point were concertedly moving, and the decreasing of the overall vdW contacts meant that the substrate was leaving the binding cavity quite slowly. The lack of a significant rupture point in the force profile suggested that the substrate did not encounter any relevant resistance despite the remarkable shift of the α3-helix. This was possible because, during the substrate pulling, the ACP α3-helix could spontaneously rearrange, allowing

the substrate exposure. This observation was supported by both free MD and experimental data,[18−26] which pointed to α3-helix as one of the most dynamic segments of ACP structure (Figure 2a).

Path 1 delivery hypothesis was then compared to path 2, to investigate if a sword-unsheathed-like mechanism could provide a flatter force profile. As shown in Figure 3d (magenta line), the unthreading of the substrate had a magnitude of forces similar to that registered for path 1b and higher than that observed in path 1c. Such a mechanism poorly complied with an ACP-enzyme interface comprising both α2-helix and its connection to α4-helix. However, a sword-unsheathed-like mechanism could be proposed for enzymes, whose interactions with ACP more extensively involve the α1-α2 loop connection.[16,20]

In summary, our simulations suggest that the substrate delivery through the cleft between α2- and α3-helix is a feasible pathway that exploits intrinsic conformational plasticity of ACP (path 1c). We also show that the ACP portion including the loop connecting helices α2 and α3 and the α3-helix itself can play a critical role in both the delivery and, as previously reported, the recognition processes.[18−26] As hypothesized on the basis of X-ray experiments,[12,15] we also point out the ability of the prosthetic group to function as a label for the acyl-intermediates carried by the ACP. Such aspects are related to ACP plasticity and may account for a mechanism in which ACP and its enzymatic counterparts minimize the solvent exposure of the lipophilic substrate moiety. The delivery model would include an ACP/enzyme interface formed by ACP helices α2 and α3; it might be hypothesized that a slight conformational change of the α3-helix could easily allow the substrate to glide into the corresponding enzyme active site.

Can we use the above uncovered features of ACP to address the development of innovative antimalarial compounds? This study sheds light on the functional and plastic features of ACP and attempts to contextualize them in the protein−protein interactions network occurring in the FAS-II system. During the elongation cycle, ACP-enzyme interactions and the delivery of the acyl substrate to the active site are compulsory steps for fatty acid production. These processes are currently the subject of drug discovery efforts. In this respect, blockers of substrate delivery would function as pathway-based antimalarial compounds rather than single FAS-II enzyme inhibitors. The design of a delivery-blocker might be achieved through a strategy that considers as template-structure for a lead-candidate that region of the α3-helix usually interacting with α2. The interaction of such a mimetic compound with *Pf*ACP would interfere with the gate opening function managed by the α2/α3 cleft. Moreover, the low-resistance delivery pathways investigated here might be used as starting point for further studies aiming at identifying local energy minima along the reaction coordinate. As a matter of fact, our simulations suggest that, while the substrate transiently leaves the carrier core moving toward the catalytic partner, the ACP core itself might become a peculiar binding pocket for small molecules able to interfere with the relocation of the substrate into the carrier. Likewise, if the conformational "transient" state of the acyl-ACP is a highly populated energy minimum, the probability to block the delivery process would dramatically increase.

ACKNOWLEDGMENT

The authors thank L. Scapozza and R. Perozzo at the University of Geneva for insightful discussions and for reading the manuscript. This research was supported by the University of Bologna.

Supporting Information Available: Methodological details, prosthetic group and substrate topology and parameters, gyration radius along the free MD simulation, effects of pulling velocity on force profiles, and expanded description of the delivery event among the paths. This material is available free of charge via the Internet at http://pubs.acs.org.

REFERENCES AND NOTES

(1) Breman, J. G. The ears of the hippopotamus: manifestations, determinants, and estimates of the malaria burden. *Am. J. Trop. Med. Hyg.* **2001**, *64*, 1–11.
(2) Greenwood, B. M.; Bojang, K.; Whitty, C. J.; Targett, G. A. Malaria. *Lancet* **2005**, *365*, 1487–1498.
(3) Snow, R. W.; Guerra, C. A.; Noor, A. M.; Myint, H. Y.; Hay, S. I. The global distribution of clinical episodes of Plasmodium falciparum malaria. *Nature* **2005**, *434*, 214–217.
(4) Surolia, A.; Ramya, T. N.; Ramya, V.; Surolia, N. 'FAS't inhibition of malaria. *Biochem. J.* **2004**, *383*, 401–412.
(5) Lu, Y. J.; Zhang, Y. M.; Rock, C. O. Product diversity and regulation of type II fatty acid synthases. *Biochem. Cell Biol.* **2004**, *82*, 145–155.
(6) White, S. W.; Zheng, J.; Zhang, Y. M.; Rock, C. O. The structural biology of type II fatty acid biosynthesis. *Annu. Rev. Biochem.* **2005**, *74*, 791–831.
(7) Shen, B.; Summers, R. G.; Gramajo, H.; Bibb, M. J.; Hutchinson, C. R. Purification and characterization of the acyl carrier protein of the Streptomyces glaucescens tetracenomycin C polyketide synthase. *J. Bacteriol.* **1992**, *174*, 3818–3821.
(8) Brozek, K. A.; Carlson, R. W.; Raetz, C. R. A special acyl carrier protein for transferring long hydroxylated fatty acids to lipid A in Rhizobium. *J. Biol. Chem.* **1996**, *271*, 32126–32136.
(9) Sweet, C. R.; Williams, A. H.; Karbarz, M. J.; Werts, C.; Kalb, S. R.; et al. Enzymatic synthesis of lipid A molecules with four amide-linked acyl chains. LpxA acyltransferases selective for an analog of UDP-N-acetylglucosamine in which an amine replaces the 3″-hydroxyl group. *J. Biol. Chem.* **2004**, *279*, 25411–25419.
(10) Kim, Y.; Prestegard, J. H. Refinement of the NMR structures for acyl carrier protein with scalar coupling data. *Proteins* **1990**, *8*, 377–385.
(11) Xu, G. Y.; Tam, A.; Lin, L.; Hixon, J.; Fritz, C. C.; et al. Solution structure of B. subtilis acyl carrier protein. *Structure* **2001**, *9*, 277–287.
(12) Roujeinikova, A.; Baldock, C.; Simon, W. J.; Gilroy, J.; Baker, P. J.; et al. X-ray crystallographic studies on butyryl-ACP reveal flexibility of the structure around a putative acyl chain binding site. *Structure* **2002**, *10*, 825–835.
(13) Wong, H. C.; Liu, G.; Zhang, Y. M.; Rock, C. O.; Zheng, J. The solution structure of acyl carrier protein from Mycobacterium tuberculosis. *J. Biol. Chem.* **2002**, *277*, 15874–15880.
(14) Sharma, A. K.; Sharma, S. K.; Surolia, A.; Surolia, N.; Sarma, S. P. Solution structures of conformationally equilibrium forms of holo-acyl carrier protein (PfACP) from Plasmodium falciparum provides insight into the mechanism of activation of ACPs. *Biochemistry* **2006**, *45*, 6904–6916.
(15) Roujeinikova, A.; Simon, W. J.; Gilroy, J.; Rice, D. W.; Rafferty, J. B.; et al. Structural studies of fatty acyl-(acyl carrier protein) thioesters reveal a hydrophobic binding cavity that can expand to fit longer substrates. *J. Mol. Biol.* **2007**, *365*, 135–145.
(16) Kim, Y.; Kovrigin, E. L.; Eletr, Z. NMR studies of Escherichia coli acyl carrier protein: dynamic and structural differences of the apo- and holo-forms. *Biochem. Biophys. Res. Commun.* **2006**, *341*, 776–783.
(17) Zhang, Y. M.; Marrakchi, H.; White, S. W.; Rock, C. O. The application of computational methods to explore the diversity and structure of bacterial fatty acid synthase. *J. Lipid Res.* **2003**, *44*, 1–10.

(18) Parris, K. D.; Lin, L.; Tam, A.; Mathew, R.; Hixon, J.; et al. Crystal structures of substrate binding to Bacillus subtilis holo-(acyl carrier protein) synthase reveal a novel trimeric arrangement of molecules resulting in three active sites. *Structure* **2000**, *8*, 883–895.
(19) Flaman, A. S.; Chen, J. M.; Van Iderstine, S. C.; Byers, D. M. Site-directed mutagenesis of acyl carrier protein (ACP) reveals amino acid residues involved in ACP structure and acyl-ACP synthetase activity. *J. Biol. Chem.* **2001**, *276*, 35934–35939.
(20) Zhang, Y. M.; Rao, M. S.; Heath, R. J.; Price, A. C.; Olson, A. J.; et al. Identification and analysis of the acyl carrier protein (ACP) docking site on beta-ketoacyl-ACP synthase III. *J. Biol. Chem.* **2001**, *276*, 8231–8238.
(21) Worsham, L. M.; Earls, L.; Jolly, C.; Langston, K. G.; Trent, M. S.; et al. Amino acid residues of Escherichia coli acyl carrier protein involved in heterologous protein interactions. *Biochemistry* **2003**, *42*, 167–176.
(22) Gong, H.; Byers, D. M. Glutamate-41 of Vibrio harveyi acyl carrier protein is essential for fatty acid synthase but not acyl-ACP synthetase activity. *Biochem. Biophys. Res. Commun.* **2003**, *302*, 35–40.
(23) Keatinge-Clay, A. T.; Shelat, A. A.; Savage, D. F.; Tsai, S. C.; Miercke, L. J.; et al. Catalysis, specificity, and ACP docking site of Streptomyces coelicolor malonyl-CoA:ACP transacylase. *Structure* **2003**, *11*, 147–154.
(24) Zhang, Y. M.; Wu, B.; Zheng, J.; Rock, C. O. Key residues responsible for acyl carrier protein and beta-ketoacyl-acyl carrier protein reductase (FabG) interaction. *J. Biol. Chem.* **2003**, *278*, 52935–52943.
(25) Zhang, L.; Liu, W.; Xiao, J.; Hu, T.; Chen, J.; et al. Malonyl-CoA: acyl carrier protein transacylase from Helicobacter pylori: Crystal structure and its interaction with acyl carrier protein. *Protein Sci.* **2007**, *16*, 1184–1192.
(26) Liu, W.; Du, L.; Zhang, L.; Chen, J.; Shen, X.; et al. Helicobacter pylori acyl carrier protein: expression, purification, and its interaction with beta-hydroxyacyl-ACP dehydratase. *Protein Expression Purif.* **2007**, *52*, 74–81.
(27) Leibundgut, M.; Jenni, S.; Frick, C.; Ban, N. Structural basis for substrate delivery by acyl carrier protein in the yeast fatty acid synthase. *Science* **2007**, *316*, 288–290.
(28) Rafi, S.; Novichenok, P.; Kolappan, S.; Zhang, X.; Stratton, C. F.; et al. Structure of acyl carrier protein bound to FabI, the FASII enoyl reductase from Escherichia coli. *J. Biol. Chem.* **2006**, *281*, 39285–39293.
(29) Izrailev, S.; Stepaniants, B. I.; Isralewitz, B.; Kosztin, D.; Lu, H.; Molnar, F.; Wriggers W.; Schulten, K. Steered molecular dynamics. In *Computational Molecular Dynamics: Challenges, Methods, Ideas*; Springer Ed.; 1999; pp 39−64.
(30) Sotomayor, M.; Schulten, K. Single-molecule experiments in vitro and in silico. *Science* **2007**, *316*, 1144–1148.
(31) MacKerell, A. D., Jr.; Bashford, D.; Bellott, M.; Dunbrack, R. L., Jr.; Evanseck, J.; et al. All-atom empirical potential for molecular modeling and dynamics studies of protein. *J. Phys. Chem. B* **1998**, *102*, 3586–3616.
(32) Phillips, J. C.; Braun, R.; Wang, W.; Gumbart, J.; Tajkhorshid, E.; et al. Scalable molecular dynamics with NAMD. *J. Comput. Chem.* **2005**, *26*, 1781–1802.
(33) Niu, C.; Xu, Y.; Luo, X.; Duan, W.; Silman, I.; et al. Dynamic mechanism of E2020 binding to acetylcholinesterase: a steered molecular dynamics simulation. *J. Phys. Chem. B* **2005**, *109*, 23730–23738.

CI800297V